

This discussion paper is/has been under review for the journal Natural Hazards and Earth System Sciences (NHESS). Please refer to the corresponding final paper in NHESS if available.

# Geohazard risk assessment using high resolution SAR interferometric techniques: a case study of Larissa National Airport Central Greece

F. Fakhri<sup>1,2</sup> and R. Kalliola<sup>1</sup>

<sup>1</sup>Department of Geography and Geology, University of Turku, 20014 Turku, Finland

<sup>2</sup>Department of Geography, Harokopio University of Athens El. Venizelou 70, 17671 Athens, Greece

Received: 23 June 2014 – Accepted: 10 July 2014 – Published: 28 July 2014

Correspondence to: F. Fakhri (falah.fakhri@utu.fi)

Published by Copernicus Publications on behalf of the European Geosciences Union.

NHESSD

2, 4743–4763, 2014

Geohazard risk assessment using high resolution SAR interferometric techniques

F. Fakhri and R. Kalliola

[Title Page](#)

[Abstract](#)

[Introduction](#)

[Conclusions](#)

[References](#)

[Tables](#)

[Figures](#)

◀

▶

◀

▶

[Back](#)

[Close](#)

[Full Screen / Esc](#)

[Printer-friendly Version](#)

[Interactive Discussion](#)

## Abstract

The possibility of use the productions of Earth Resource Satellite (ERS-1/2) and Advanced Environment Satellite ENVISAT SAR (Synthetic Aperture Radar) C-band have given the potential to detect and estimate the time series of dynamic ground deformation within high spatial and temporal resolution. The Larissa National Airport is suffering from continued ground deformation as evidenced by the presence of ground fissures and sinkholes as well as observed land subsidence. This study uses two Synthetic Aperture Radar interferometric techniques (InSAR) to detect short- and long-term ground deformation dynamics in the airport using the GAMMA Software (S/W). The results indicate complex subsidence and uplift processes at ranges between  $-15$  and  $25 \text{ mm a}^{-1}$  to co-occur in different parts of the study region. Some of these changes may be attributed to tectonic fault movements but some of the observed ground deformation processes are more likely to result from human induced changes in the ground-water level and expansive soils.

## 15 1 Introduction

Ground movement is a major cause of natural hazards that threaten the stability of civil and agricultural infrastructures. This reality imposes a need to monitor and estimate dynamic ground movements with high spatial and temporal resolutions. The current study focuses the region of Thessaly in central Greece where various types of co-  
20 occurring ground deformation changes damage the region's important infrastructures. Numerous fissures may open up across the Thessaly Plain during the dry season mainly at its eastern parts, cutting across cultivated land, roads, houses, and even the area of the Larissa National Airport where fissures up to several tens of centimeters may form, presenting also an expansion rate of up to  $30 \text{ mm a}^{-1}$  (Kontogianni et al.,  
25 2007). Unstable ground affects significantly and directly the runways and may threaten takeoff and landing security.

NHESSD

2, 4743–4763, 2014

---

## Geohazard risk assessment using high resolution SAR interferometric techniques

F. Fakhri and R. Kalliola

---

[Title Page](#)

[Abstract](#)

[Introduction](#)

[Conclusions](#)

[References](#)

[Tables](#)

[Figures](#)

◀

▶

◀

▶

[Back](#)

[Close](#)

[Full Screen / Esc](#)

[Printer-friendly Version](#)

[Interactive Discussion](#)

---

**Geohazard risk assessment using high resolution SAR interferometric techniques**

F. Fakhri and R. Kalliola

[Title Page](#)[Abstract](#)[Introduction](#)[Conclusions](#)[References](#)[Tables](#)[Figures](#)[◀](#)[▶](#)[◀](#)[▶](#)[Back](#)[Close](#)[Full Screen / Esc](#)[Printer-friendly Version](#)[Interactive Discussion](#)

The opening of these fissures may be related to drought and over-exploitation of groundwater. For example the South Ring Expressway and Wushu International Airport in the southern suburb of Taiyuan, China, are being threatened by severe ground subsidence due to groundwater overexploitation (Wu et al., 2010). Groundwater it is also the dominant process driving land subsidence in the region of Morelia in Mexico, also resulting in shallow faulting which mimics pre-existing faults, possibly with minor contributions from present-day tectonics (Chang et al., 2004; Cigna et al., 2011; Raspini et al., 2013).

In a previous SAR interferometry study in the region of Thessaly reflecting the period from 1992 to 2006 by Lagios (2007), it was found that systematic subsidence is the predominant feature in the region, reaching maximum amplitude of about 350 mm (Gianouli area). However, the Larissa city center appears to be geophysically stable compared to its northern and eastern suburbs, which are closer to cultivated regions. Using SAR techniques to detect seasonal deformation signals in the south-western part of the southern part of the Thessaly Plain, Parcharidis et al. (2011) detected vertical changes up to several centimeters during the summer period. Fakhri (2013) and Fakhri and Kalliola (2014) used enhanced interferometric techniques to study ground deformation with higher precision and in different timescales, and found both short- and long- term ground deformation processes to co-occur at the regional scale.

In the present study we apply spatially and temporally high precision enhanced SAR interferometric techniques to monitor ground deformation dynamics and to evaluate the geohazard risk that corresponds in the area of the Larissa National Airport. Furthermore we will reveal whether this ground deformation is likely to be resulting from short- or/and long- term impacts of groundwater level fluctuations through the swelling and shrinkage operations of clay minerals.

## 2 Study area

The Larissa National Airport is located in the Eastern part of Larissa in the northern Thessaly region in Central Greece (Fig. 1). It was built in 1912 and functioned as the main airport of the city until 1997 when it was closed from civil uses. Currently it still serves as a military airport.

Considerable neo-tectonic activity occurs in the region; the known active faults are normal and WNW-trending, indicating a NNE extension (Caputo, 1993). The Rodia fault system in the northern part of the Larissa basin is composed of several segments characterized by different directions and ages, having a general E–W to ESE–WNW direction and finally bounding to the north to Tyrnavos Low where the Palaeozoic substratum is in direct contact with Pliocene and mainly Quaternary deposits. Thessaly, both in general and in particular in the sector corresponding to the Tyrnavos Basin, as well as most of the villages in the region, are settled on thick Quaternary fluvio-lacustrine deposits and therefore on highly vulnerable geological conditions for the possible occurrence of site effects (Caputo, 1993; Caputo and Helly, 2005).

The precipitation in the study area shows both monthly, seasonal and inter-annual variations (Fig. 2). The minimum precipitation during the summer season is close to zero whereas the maximum is over 90 mm. Precipitation levels during winter are in general higher yet variable between the years. The major aquifers within the graben are composed of coarse grained permeable sediments with locally interbedded layers of silt and clay up to 300 m thick (Petalas et al., 2005).

Both of the two major basins in the region, the Pinios River basin and the Lake Karla basin, are extensively used for intensive cultivation of water-demanding crops, such as cotton and maize. The absence of reasonable water resources management has led to a remarkable increase in water demand, which is usually fulfilled by the over-exploitation of groundwater resources. This unsustainable practice has deteriorated the already disturbed water balance and accelerated water resources degradation leading

[Title Page](#)

[Abstract](#)

[Introduction](#)

[Conclusions](#)

[References](#)

[Tables](#)

[Figures](#)

◀

▶

◀

▶

[Back](#)

[Close](#)

[Full Screen / Esc](#)

[Printer-friendly Version](#)

[Interactive Discussion](#)

in some cases into seawater intrusion or land subsidence (Loukas et al., 2007; Rozos et al., 2010).

The Pineios River basin where the Larissa National Airport is located also suffers serious water shortage due to poor water resources management and the increasing demand for water. In order to identify and to estimate the relation of groundwater level fluctuation on land deformation, more than 15 wells have been established in the region by the Thessaly Larissa Regional Unit (Decentralized Administration of Thessaly Sterea Elada). One of these boreholes is located 100 m east of the Larissa National Airport and its data are here used to construct a sequence of groundwater level fluctuations for the study area along the time axis for the period 1992–2010.

### 3 SAR data and methods

Ground deformation was monitored by the use of 24 Single Look Complex (SLC) SAR C-band images of ERS-1/2, during 1995–2000 and 15 SLC images of ENVISAT ASAR acquired during 2003–2008 by ESA (Table 1). The examined time period extends from 1995 till 2008 (13 years).

Two SAR interferometric techniques were used with the GAMMA processing software (S/W) (Gamma Remote Sensing, 2008). A conventional technique of SAR interferometry was implemented to investigate short term patterns of ground deformation and to ascertain whether they are attributable to the locations of faults or are likely to originate due to any other impact factor. In such Differential InSAR approach, the effects of surface topography and coherent displacement can be separated. The retrieval of displacement maps is facilitated by combining multiple observations into an interferogram that has the potential to provide millimeter scale accuracy (Ferretti et al., 1999).

Persistent Scatters Technique was applied to identify ground deformation in relation to long term groundwater level fluctuations. This technique relies on identifying selected ground elements that are dominated by a single scatterer and involve interferometric

[Title Page](#)

[Abstract](#)

[Introduction](#)

[Conclusions](#)

[References](#)

[Tables](#)

[Figures](#)

◀

▶

◀

▶

[Back](#)

[Close](#)

[Full Screen / Esc](#)

[Printer-friendly Version](#)

[Interactive Discussion](#)

phase comparison of SAR images gathered at different times. The use of the interferometric phase from long time data series requires that the correlation remains high over the entire observation period (Fruneau et al., 2003; Wegmüller et al., 2006; Hooper, 2006; Agram, 2010; Ferretti et al., 1999; Werner et al., 2003). Although temporal correlation and atmospheric inhomogeneities may occur, reliable deformation measurements at the scale of millimeters can be obtained in a multi-image framework on a small subset of image pixels corresponding to stable areas. These points, hereafter called Permanent Scatterers (PS), provide a kind of natural network of ground control points to monitor terrain motion through the phase history of each one. Interferometric Point Target Analysis (IPTA) was furthermore used to assess the temporal and spatial characteristics of interferometric signatures from point targets that exhibit long-term coherence. The processing proceeded by performing a least-squares regression on the differential phase to estimate height and deformation rate (see Werner et al., 2003). The estimates are relative to a reference point in the scene.

## 4 Results

### 4.1 Behavior of the groundwater level

Time series data of the groundwater level indicates fluctuations resulting from the mutual recharge and discharge of the aquifer and a continuous decline towards the end of the monitored period (Fig. 3). Groundwater level tends to rise during the late fall, is high during winter and early spring, lowers in late spring and is at low level during summer. The months of May and October often show rapid changes in groundwater level.

## Geohazard risk assessment using high resolution SAR interferometric techniques

F. Fakhri and R. Kalliola

[Title Page](#)

[Abstract](#)

[Introduction](#)

[Conclusions](#)

[References](#)

[Tables](#)

[Figures](#)

◀

▶

◀

▶

[Back](#)

[Close](#)

[Full Screen / Esc](#)

[Printer-friendly Version](#)

[Interactive Discussion](#)



## 4.2 Ground deformation according to SAR interferometry

### 4.2.1 Short term changes

Conspicuous patterns can be observed in the conventional SAR Inferometry images of the study area (Fig. 4). The perpendicular baseline in these analyses during the 5 wintertime (Fig. 4a) is small ( $B^\perp$  –66.80 m) to avoid residual topographic effects and geometric de-correlation. The subsidence phase around the borehole and along most of the runways and especially the density of the subsidence phase to the north and east of the borehole are probably due to low groundwater level, since the depth of groundwater level was low (20.62 m) and the normalized subsidence deformation rate 10 LOS (Line of Sight) was –62 mm. In the summertime analyses (Fig. 4b) the perpendicular baseline was too small for a precise analysis ( $B^\perp$  –1.51 m). Clear interferometric fringes can anyhow be directed around the borehole SR72 and along all runways, indicating subsidence that may be related to the lowering groundwater level (34.00 m) during the monitored part of the dry period.

### 15 4.2.2 Long term changes

The persistent scatterers inferometry covering the time period from 1995 to 2006 contains 236 candidate points (Fig. 5). Their change patterns indicate subsidence deformation at rates varying between –1 to –15 mm LOS<sup>–1</sup> as well as uplift deformation up to 25 mm LOS<sup>–1</sup>. Three candidate points were chosen examine temporal changes in 20 groundwater level and land deformation.

The point number 41694 which is located 322 m from the borehole R72 indicates a general rising trend after a short initial period of subsidence (Fig. 6a). The minimum and maximum subsidence rates were 3.059 mm in April 2004 and –149.104 mm in June 1995, respectively, while the minimum and maximum uplift rates were 3.712 mm in 25 May 2005 and 33.334 mm in December of 2006, respectively. The deformation behavior of the point number 41858, at a distance of 341 m from the borehole R72, also indicates

[Title Page](#)

[Abstract](#)

[Introduction](#)

[Conclusions](#)

[References](#)

[Tables](#)

[Figures](#)

◀

▶

◀

▶

[Back](#)

[Close](#)

[Full Screen / Esc](#)

[Printer-friendly Version](#)

[Interactive Discussion](#)

a general rising trend, as the time series begins with subsidence and then goes into uplift.

The deformation behavior of the third point (number 41185), at a distance of 475 m from the borehole R72, shows rather equal deformation behavior but the change rate as the beginning of the monitored period was lower. There was a swap between subsidence and uplift during the period April 2004–May 2005 and eventually uplift is observed. The minimum and maximum subsidence was  $-1.971\text{ mm}$  in April 2004 and  $-75.945\text{ mm}$  in December 1995, respectively, while the minimum and maximum uplift was  $0.881\text{ mm}$  in August 2004 and  $18.254\text{ mm}$  in December 2006 respectively.

## 10 5 Discussion

Both of the applied SAR interferometric techniques revealed relatively fast but highly site specific ground deformation in and around the Larissa National Airport. Conventional SAR interferometry showed seasonally varying spatial change patterns over the study area whereas the persistent scatterer interferometry indicated longer term dynamics with centimeter level annual changes and an overall trend of uplift.

In a study using archive data stack (3 m resolution) from 17 RADARSAT-2 images in the Iqaluit Airport in NE Canada, locally inhomogeneous ground uplift has been shown to cause cracking and bending of the runway (Cusson et al., 2012). Fast subsidence has also been documented by differential InSAR (DInSAR) technique near the 15 Vancouver International Airport and Sky Train station (Samsonov et al., 2014). Persistent scatterers, in turn, have shown both subsidence and uplift in the Belgian National Airport of Zaventem (Devleeschouwer et al., 2006), moderate subsidence exceeding  $-20\text{ mm a}^{-1}$  in the Tucson city in Arizona (Cusson et al., 2012; Kim, 2013), and ground deformation along the wider coastal zone including the airport area of the Anthemountas basin in northern Greece (Raspini et al., 2013). Such spatially and temporally variable ground deformation dynamics in sedimentary basins can often be associated with intense groundwater extraction within the region (Chang et al., 2004; Wu et al., 2010;

[Title Page](#)

[Abstract](#)

[Introduction](#)

[Conclusions](#)

[References](#)

[Tables](#)

[Figures](#)

◀

▶

◀

▶

[Back](#)

[Close](#)

[Full Screen / Esc](#)

[Printer-friendly Version](#)

[Interactive Discussion](#)

Cigna et al., 2011; Raspini et al., 2013; Samsonov et al., 2014). Earth fissures, the most spectacular manifestation of subsidence-related phenomena, often occur near the margins of alluvial basins, exposed or shallow buried bedrock, or over zones of changing alluvial basin characteristics (facies).

- 5 Subsidence attributed to aquifer-system compaction in the USA is generally largest in magnitude and distribution in the western aquifer systems and in the Houston area of the Coastal lowlands aquifer system (Galloway and Sneed, 2013). The susceptibility of these aquifer systems to aquifer-system compaction is enhanced because of the large groundwater abstractions and the prevalence of fine-grained (clays and silts)  
10 deposits. By virtue of their larger compressibility's under virgin (inelastic) loading conditions, compaction of the fine-grained sediments causes subsidence.

Declined ground water level may also act as a carrier of small granular soil particles, which may stimulate the process of ground or soil compaction. The transport of suspended particulate matter is widely recognized to occur in subsurface environments.

- 15 Field data indicate that viruses, bacteria, colloids and clay particles can migrate considerable distances until the groundwater (McDowell-Boyer, 1986; Gschwend et al., 1990). All changes that modify soil volume may pose hazard to engineering construction as they can cause heaving or shrinkage of structures. However, these expansive effects may become "diluted" by the presence of abundant non-swelling minerals in  
20 soil structure, such as quartz and carbonates (Jones and Jefferson, 2011; Mokhtari and Dehghani, 2012).

The dynamic and spatially variable nature of ground deformation in the Larissa National Airport, as documented in this study, suggests that the excessive and intensive groundwater withdrawal in the region is likely to be the main engine of such changes.

- 25 This view is supported by the fact that in the eastern, western, northeastern, southern, and southwestern regions of the eastern part of northern Thessaly, the swelling clay minerals of montmorillonite and illite are widely present in the surface soil structure, from 0 to 16.1 % and from 17.6 to 30.4 %, respectively (Sgouras, 1994). However,

---

## Geohazard risk assessment using high resolution SAR interferometric techniques

F. Fakhri and R. Kalliola

---

[Title Page](#)

[Abstract](#)

[Introduction](#)

[Conclusions](#)

[References](#)

[Tables](#)

[Figures](#)

[◀](#)

[▶](#)

[◀](#)

[▶](#)

[Back](#)

[Close](#)

[Full Screen / Esc](#)

[Printer-friendly Version](#)

[Interactive Discussion](#)

the potential contribution of simultaneous micro-tectonic changes through pre-existing faults cannot be fully excluded.

## 6 Conclusions

The possibility of use the productions of Earth Resource Satellite (ERS-1/2) and Advanced Environment Satellite ENVISAT SAR (Synthetic Aperture Radar) C-band have given the potential to monitor, detect and estimate the ground deformation during long- and short-term and also assess the time series of dynamic ground deformation within high spatial and temporal resolutions. The combined use of two different InSAR techniques resulted in spatially and temporally accurate monitoring of ground deformation dynamics in Larissa National Airport. Probably the most important factors causing such changes are the impacts of the swelling and shrinkage of clay minerals (expansive soil), which can be activated through groundwater withdrawal and recharge.

## Authors contributions

Falah Fakhri designed the research parameters and performed the research and collected the reference data; Risto Kalliola has reviewed the results, Risto Kalliola and Falah Fakhri authored the manuscript.

*Acknowledgements.* The authors would like to acknowledge the European Space Agency (ESA) for providing the ERS\_1/2, ENVISAT ASAR data. Greatly acknowledge also; Issaak Parcharidis for his comments and suggestions significantly improved an earlier version of this manuscript. UTU

## References

- Agram, P. S.: Persistent Scatterer Interferometry in Natural Terrain, PhD thesis, Stanford University, Department of Electrical Engineering, Stanford, 2010.
- ALSG: Land Subsidence and Earth Fissures in Arizona, Arizona Geological Survey, Arizona, 2007.
- 5 Caputo, R.: The Rodia Fault System; an Active Complex Share Zone (Larissa Plain, Central Greece), *Bull. Geol. Soc. Am.*, **Xxviii/1**, 447–456, 1993.
- Caputo, R. and Helly, B.: The Holocene Activity of the Rodi'A Fault Central Greece, *Geodynamics*, **40**, 153–169, 2005.
- 10 Chang, C. P., Chang, T. Y., Wang, C. T., Kuo, C. H., and Chen, K. S.: Land-surface deformation corresponding to seasonal ground-water fluctuation, determining by SAR interferometry in the SW Taiwan, *Math. Comput. Simulat.*, **67**, 351–359, 2004.
- Cigna, F., Osmanoğlu, B., Cabral-Cano, E., Dixon, T. H., Alejandro, J., Ávila-Olivera, J. A., 15 Garduño-Monroy, V. H. G., Demets, C., and Wdowinski, S.: Monitoring land subsidence and its induced geological hazard with synthetic aperture radar interferometry: a case study in Morelia, Mexico, *Remote Sens. Environ.*, **117**, 146–161, 2011.
- Cusson, D., Ghuman, P., Gara, M., and McCardle, A.: Remote monitoring of bridges from space, *Anais do 54º Congresso Brasileiro do Concreto – CBC2012 – 54CBC*, IBRACON, 1–25, 2012.
- 20 Decentralized Administration of Thessaly Sterea Elada: available at: <http://www.larissa.gr/main.aspx?catid=98&dnsi=21&tm=47> (last access: March 2012), Direction of Water Management of Thessaly, Department of Water Resource Monitoring and Protection for the Region of Thessaly, Larissa, 2011.
- Devleeschouwer, X., Pouriel, F., and Declercq, P.-Y.: Vertical displacements (uplift) revealed by the PSInSAR technique in the centre of Brussels, Belgium, *The Geological Society of London, London*, 1–10, 2006.
- 25 Fakhri, F.: Long and Short Term Monitoring of Ground Deformation in Thessaly Basin Using Space-Based SAR Interferometry, Ph.D. thesis, Department of Geography Harokopio University of Athens, Athens, 2013.
- 30 Fakhri, F. and Kalliola, R.: Monitoring ground deformation in the settlement of Larissa in central Greece by implementing SAR interferometry, *Nat. Hazards*, in review, 2014.

[Title Page](#)

[Abstract](#)

[Introduction](#)

[Conclusions](#)

[References](#)

[Tables](#)

[Figures](#)

◀

▶

◀

▶

[Back](#)

[Close](#)

[Full Screen / Esc](#)

[Printer-friendly Version](#)

[Interactive Discussion](#)

**Geohazard risk assessment using high resolution SAR interferometric techniques**

F. Fakhri and R. Kalliola

- 5 Ferretti, A., Prati, C., and Rocca, F.: Permanent scatterers in SAR interferometry, in: Int. Geosci. Remote Sensing Symp., Hamburg, Germany, 1999.
- 10 Fruneau, B., Deffontaines, B., Rudant, J. P., Parmentier, A. M. L., Colesanti, C., Mouelic, S. L., Carne, C., and Ferretti, A.: Conventional and PS differential SAR interferometry for monitoring vertical deformation due to water pumping the Haussmann–St-Lazare case example, Fringe Workshop, Frascati, Italy, 2003.
- 15 Galloway, D. and Sneed, M.: Analysis and simulation of regional subsidence accompanying groundwater abstraction and compaction of susceptible aquifer systems in the USA, Boletín de la Sociedad Geológica Mexicana, 65, 123–136, 2013.
- 20 10 Gamma Remote Sensing: Documentation – User's Guide, Differential Interferometry and Geocoding Software – Diff & Geo. 1.2 Ed., Gamma Remote Sensing AG, Gumiingen, Switzerland, 2008.
- 25 Gschwend, P., Backhus, A. D., MacFarlane, J. K., and Page, A. L.: Mobilization of colloids in groundwater due to infiltration of water at a coal ash disposal site, J. Contam. Hydrol., 6, 307–320, 1990.
- 30 15 Hellenic National Meteorological Service HNMS: available at: <http://www.hnms.gr>, last access: 25 January 2014.
- 20 Hooper, A. J.: Persistent Scatterer Radar Interferometry for Crustal Deformation Studies and Modeling of Volcanic Deformation, Ph.D. thesis, Stanford University, Department of Geophysics, Stanford, 2006.
- 25 Jones, L. D. and Jefferson, I.: Expansive Soils, Institution of Civil Engineers Manuals Series available at: [http://nora.nerc.ac.uk/17002/1/C5\\_expansive\\_soils\\_Oct.pdf](http://nora.nerc.ac.uk/17002/1/C5_expansive_soils_Oct.pdf) (last access: February 2014), 2011.
- 30 25 Kim, J. W.: Applications of Synthetic Aperture Radar (SAR)/SAR interferometry (InSAR) for Monitoring of Wetland Water Level and Land Subsidence, Geodetic Science, The Ohio State University, Columbus, Ohio, 2013.
- 35 Kontogianni, V., Pytharouli, S., and Stiros, S.: Ground subsidence, Quaternary faults and vulnerability of utilities and transportation networks in Thessaly, Environ. Geol., 52, 1085–1095, 2007.
- 40 Lagios, E.: Long term and seasonal ground deformation monitoring of Larissa plain (central Greece), Initial Interpretation Report Prepared for Esa Gmes, Ps InSAR, s.l., Athens, Terafirma National and Kapodistrian University of Athens, School of Science, Faculty of Geology and Geoenviroment, Department of Geophysics and Geothermic, Athens, 2007.

[Title Page](#)[Abstract](#)[Introduction](#)[Conclusions](#)[References](#)[Tables](#)[Figures](#)[◀](#)[▶](#)[◀](#)[▶](#)[Back](#)[Close](#)[Full Screen / Esc](#)[Printer-friendly Version](#)[Interactive Discussion](#)

Loukas, A., Mylopoulos, N., and Vasiliades, L.: A modeling system for the evaluation of water resources management strategies in Thessaly, Greece Water Resources Manage., 21, 1673–1702, 2007.

5 McDowell-Boyer, L. M., Hunt, J. R., and Sitar, N.: Particle transport through porous media, Water Resour. Res., 22, 1901–1921, 1986.

Mokhtari, M. and Dehghani, M.: Swell-shrink behavior of expansive soils, damage and control, Elect. J. Geotech. Eng., 17, 2673–2682, 2012.

10 Parcharidis, I., Foumelis, M., and Katsafados, P.: Seasonal ground deformation monitoring over southern Larissa plain (central Greece) by SAR interferometry, Environ. Earth Sci., 2, 497–504, 2011.

Petalas, C., Pisinaras, V., Koltsida, K., and Tsirhrintzis, V. A.: The Hydrological Regime of the East Basin of Thessaly, Rhodes Island, Greece, 9th International Conference on Environmental Science and Technology, Rhodes, 2005.

15 Raspini, F., Loupasakis, C., Rozos, D., and Moretti, S.: Advanced interpretation of land subsidence by validating multi-interferometric SAR data: the case study of the Anthemountas basin (Northern Greece), Nat. Hazards Earth Syst. Sci., 13, 2425–2440, doi:10.5194/nhess-13-2425-2013, 2013.

20 Rozos, D., Sideri, D., Loupasakis, C., and Apostolidis, E.: Land Subsidence Due to Excessive Groundwater Withdrawal. A Case Study From Stavros – Farsala Site, West Thessaly, Patras Greece, 12th International Congress, Greece, Bulletin of the Geological Society Of Greece, 2010.

25 Samsonov, V. S., d'Oreye, N., González, P. J., and Tiampo, K. F.: Rapidly accelerating subsidence in the Greater Vancouver region from two decades of ERS-ENVISAT-RADARSAT-2 DInSAR measurements, Remote Sens. Environ., 143, 180–191, 2014.

Sgouras, I.: Relationship of Calcareous Geological Substrate With the Properties of Overburden Soil, Ph.D. thesis, Department of Land Improvement and Agricultural Engineering, Agricultural University of Athens, Athens, 1994.

30 Wang, G. Y., You, G., Shi, B., Yu, J., Li, H. Y., and Zong, K. H.: Earth fissures triggered by groundwater withdrawal and coupled by geological structures in Jiangsu Province, China, Environ. Geol., 57, 1047–1054, 2009.

Wegmüller, U., Werner, C., Strozzi, T., and Wiesmann, A.: Application of SAR Interferometric Techniques for Surface Deformation Monitoring, 3rd. Baden, IAG, 12th Fig Symposium, Baden, 2006.

## Geohazard risk assessment using high resolution SAR interferometric techniques

F. Fakhri and R. Kalliola

[Title Page](#)

[Abstract](#)

[Introduction](#)

[Conclusions](#)

[References](#)

[Tables](#)

[Figures](#)

◀

▶

◀

▶

[Back](#)

[Close](#)

[Full Screen / Esc](#)

[Printer-friendly Version](#)

[Interactive Discussion](#)

Werner, C., Wegmüller, U., Wiesmann, A., and Strozzi, T.: Interferometric Point Target Analysis With Jers-1 L-Band SAR Data, Igars'03, Toulouse, France, 2003.

Wu, H., Zhang, Y., Zhang, J., and Chen, X.: Mapping Deformation of Man-Made Linear Features Using Dinsar Technique, XXXVIII, Part 7A, ISPRS TC VII Symposium, Vienna, Austria, 2010.

**NHESSD**

2, 4743–4763, 2014

---

**Geohazard risk assessment using high resolution SAR interferometric techniques**

F. Fakhri and R. Kalliola

---

[Title Page](#)

[Abstract](#)

[Introduction](#)

[Conclusions](#)

[References](#)

[Tables](#)

[Figures](#)

◀

▶

◀

▶

[Back](#)

[Close](#)

[Full Screen / Esc](#)

[Printer-friendly Version](#)

[Interactive Discussion](#)

**Table 1.** Datasets of ERS-1/2 SAR images (Ascending Track 143, Frame 785) and ENVISAT ASAR SAR images (Ascending Track 143, Frame 783) used in the processing.

Missions	Acquisition Date	Orbit	B <sup>⊥</sup> (m)
ERS1	28 Jun 1995	20672	615.44
ERS1	20 Dec 1995	23177	-355.38
ERS1	28 Feb 1996	24179	-273.99
ERS1	3 Apr 1996	24680	-340.82
ERS1	8 May 1996	25181	-633.79
ERS1	20 Oct 1999	43217	-114.30
ERS2	29 Jun 1995	00999	760.036
ERS2	21 Dec 1995	03504	-355.38
ERS2	29 Feb 1996	04506	-720.395
ERS2	4 Apr 1996	05007	-215.33
ERS2	9 May 1996	05508	-517.27
ERS2	20 Mar 1997	10017	292.54
ERS2	29 May 1997	11019	156.397
ERS2	7 Aug 1997	12021	276.35
ERS2	25 Dec 1997	14025	-649.843
ERS2	9 Apr 1998	15528	637.29
ERS2	18 Jun 1998	16530	159.16
ERS2	27 Aug 1998	17532	-242.85
ERS2	14 Jan 1999	19536	137.424
ERS2	29 Apr 1999	21039	394.86
ERS2	3 Jun 1999	21540	-389.10
ERS2	21 Oct 1999	23544	125.55
ERS2	18 May 2000	26550	601.616
ENVISAT	3 Apr 2003	05708	866.89
ENVISAT	21 Aug 2003	07712	281.569
ENVISAT	8 Jan 2004	07712	-769.243
ENVISAT	12 Feb 2004	10217	-370.97
ENVISAT	22 Apr 2004	11219	-627.5.0
ENVISAT	27 May 2004	11720	-595.195
ENVISAT	5 Aug 2004	12722	330.509
<b>*ENVISAT</b>	<b>9 Sep 2004</b>	<b>13223</b>	<b>0.000</b>
ENVISAT	14 Oct 2004	13724	-1012.07
ENVISAT	12 May 2005	16730	-460.2.3
ENVISAT	25 Aug 2005	18233	426.83
ENVISAT	28 Dec 2006	25247	397.01
ENVISAT	1 Feb 2007	25748	-316.94
ENVISAT	27 Mar 2008	31760	304.81
ENVISAT	5 Jun 2008	32762	420.258

Master image (IPTA technique).

**Geohazard risk assessment using high resolution SAR interferometric techniques**

F. Fakhri and R. Kalliola

[Title Page](#)

[Abstract](#)

[Introduction](#)

[Conclusions](#)

[References](#)

[Tables](#)

[Figures](#)

◀

▶

◀

▶

[Back](#)

[Close](#)

[Full Screen / Esc](#)

[Printer-friendly Version](#)

[Interactive Discussion](#)



**Figure 1. (a)** Location of the study area and geological map of the Larissa region as modified from IGME – Greek Institute of Geology and Mineral Exploration <http://www.managenergy.net/actors/1337>. Normal faults are digitized according to Caputo et al. (1993, 2005). **(b)** Landsat TM image of Larissa and its vicinities. **(c)** Landsat TM image of the Larissa National Airport. Sources of the Landsat images: USGS <http://landsat.usgs.gov/landsat8.php>.

## Geohazard risk assessment using high resolution SAR interferometric techniques

F. Fakhri and R. Kalliola

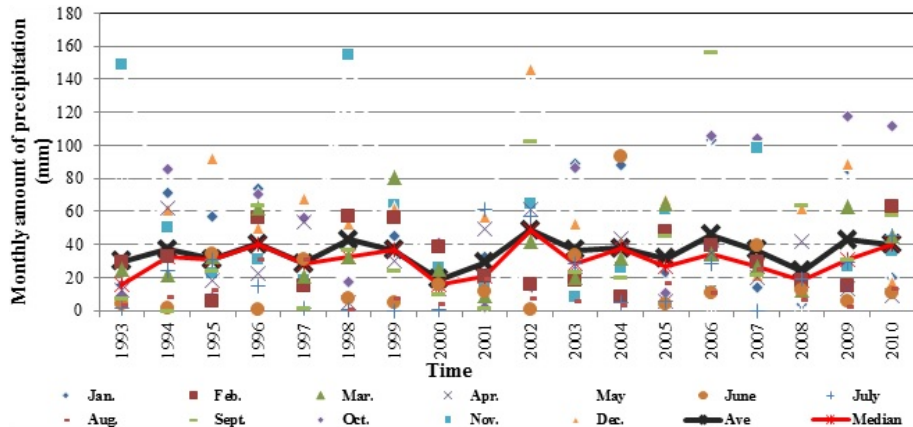


**Figure 2.** Monthly precipitations (point symbols) and the year-wise averages and medians of monthly precipitations for the period 1992–2010. The data is from the Larissa meteorological station which is operated by the Hellenic national meteorological service HNMS.

- [Title Page](#)
- [Abstract](#) [Introduction](#)
- [Conclusions](#) [References](#)
- [Tables](#) [Figures](#)
- [◀](#) [▶](#)
- [◀](#) [▶](#)
- [Back](#) [Close](#)
- [Full Screen / Esc](#)
- [Printer-friendly Version](#)
- [Interactive Discussion](#)

## Geohazard risk assessment using high resolution SAR interferometric techniques

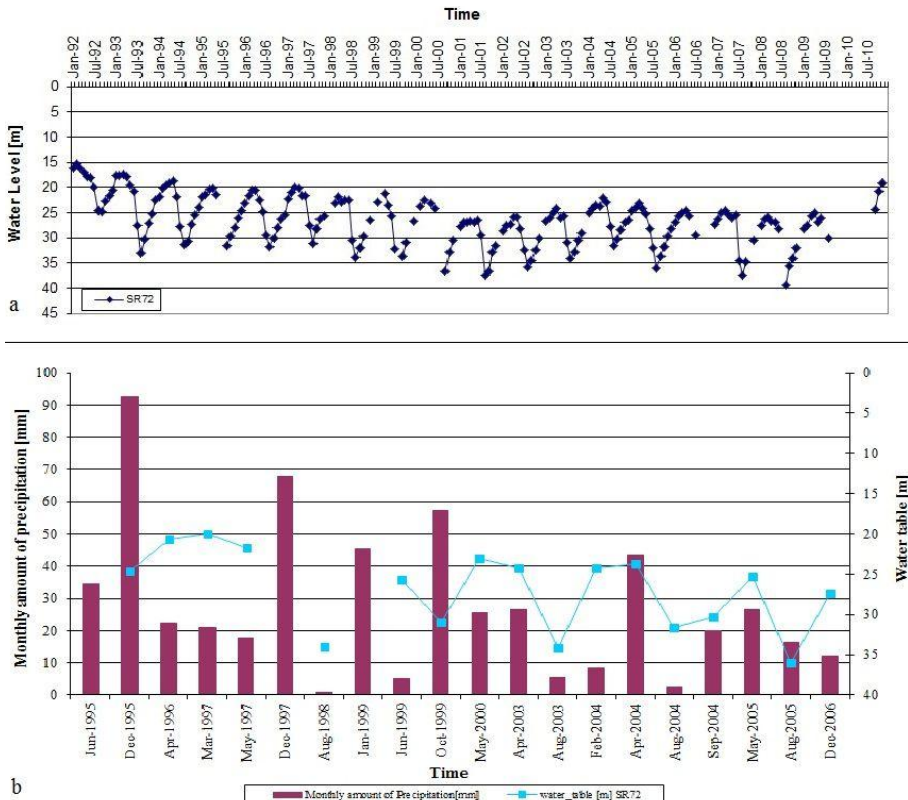


**Figure 3.** Hydrographical time series data from the study area. **(a)** Fluctuations of groundwater level for borehole SR72 during the period 1992–2010. **(b)** Average precipitation and groundwater levels of selected months during the period 1992–2010.

4760

# Geohazard risk assessment using high resolution SAR interferometric techniques

F. Fakhri and R. Kalliola

Figure 1 consists of two panels, (a) and (b), showing SAR interferograms of a geological area. Both panels include a color bar for normalized LOS deformation rate, a scale bar (0-800 meters), and a north arrow.

**Panel (a):** Shows a normalized LOS deformation rate of 57 mm. The color bar ranges from -62 to 57 mm. The interferogram displays various geological features, including a prominent linear feature and several smaller, irregularly shaped areas of high deformation.

**Panel (b):** Shows a normalized LOS deformation rate of 63 mm. The color bar ranges from -163 to 63 mm. This panel also shows similar geological features to panel (a), with a linear feature and several high-deformation areas.

**Figure 4.** Two conventional InSAR interferogram images of the study area. **(a)** Representing the period from 28 February 1996 to 3 April 1996 within the track 143. **(b)** The period from 2 August 1998 to 6 September 1998 within the descending track 279. The position of the groundwater borehole well SR72 is shown with white point.

4761

A small rectangular icon with a grey border. Inside, on the left, is a white circle with 'CC' in black. On the right is another white circle with a black silhouette of a person. Below the person icon is the text 'BY'.

## Geohazard risk assessment using high resolution SAR interferometric techniques

F. Fakhri and R. Kalliola



**Figure 5.** Average LOS velocity image along the runway and areas of Larissa National Airport for the period 1995 to 2006. The image has been saturated at  $\pm 0.1 \text{ m year}^{-1}$  for visualization purposes. The numbered persistent scatterers with cyan color have been extracted and analyzed to evaluate time series of ground deformation. Background is base map world imagery white point is the borehole R72.

Title Page

## Abstract

## Introduction

## Conclusions

## References

## Tables

## Figures

1

▶

1

▶

## Back

Close

Full Screen / Esc

### Interactive Discussion

## Geohazard risk assessment using high resolution SAR interferometric techniques

F. Fakhri and R. Kalliola

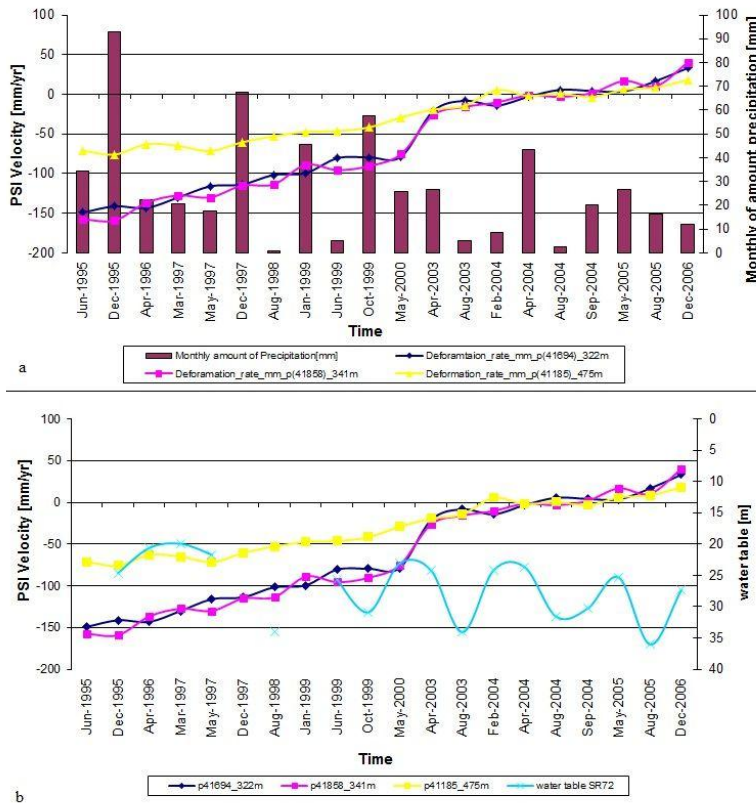


**Figure 6.** LOS Displacement of three candidate points of PSI. **(a)** Corresponding to monthly precipitation. **(b)** Corresponding to groundwater level of borehole SR72. Displacement time series of point candidates are rescaled to the first acquisition (i.e. 28 June 1995).